UNCLASSIFIED

AD 667 491

THE MECHANICAL PROPERTIES OF THE CORROSION PRODUCT FORMED DURING OXIDATION OF COPPER

Billy W. Sloope

Virginia Institute for Scientific Research
Richmond, Virginia

2 April 1968

Processed for . . .

DEFENSE DOCUMENTATION CENTER
DEFENSE SUPPLY AGENCY

CLEARINGHOUSE
FOR FEDERAL SCIENTIFIC AND TECHNICAL INFORMATION

U. S. DEPARTMENT OF COMMERCE / NATIONAL BUREAU OF STANDARDS / INSTITUTE FOR APPLIED TECHNOLOGY

AD 667491

Final Report

"The Mechanical Properties of the Corrosion Product Formed during Oxidation of Copper"

ONR Contract No. N00014-66-C0182

Period Covered:
1 April, 1966 - 31 March, 1968

Reproduction in whole or in part is permitted for any purpose of the United States Government. Research was sponsored by The Office of Naval Research. ONR Contract Authority identification number is NR 036-066/2-16-66.

Distribution of this document is unlimited.

APR 15 1968

Dr. Billy W. Sloope

Virginia Institute for Scientific Research
P. O. Box 8315
Richmond, Virginia 23226

April 2, 1968

Reproduced by the
CLEARINGHOUSE
for Federal Scientific & Technical
Information Springfield Va 22151

TABLE OF CONTENTS

	Page
INTRODUCTION	2
EXPERIMENTAL	4
Sample Preparation	4
Thickness Measurements	5
Bulge Apparatus	7
Results: Cu Films	9
Oxidized Cu Films	16
CONCLUSIONS AND DISCUSSION	25
ACKNOWLEDGMENT	27
PUBLICATIONS AND TALKS RESULTING FROM RESEARCH	27
APPENDICES	
APPENDIX A. Mathematical Evaluation of Bulge Technique	A1
APPENDIX B. Experimental Evaluation of the Bulge Technique	B1
APPENDIX C. The Mechanical Properties of Oxidized Single Crystal Copper	C1

INTRODUCTION

The objective of this research is the determination of the mechanical properties of the oxide corrosion product formed on copper. Two lines of approach have been followed: (1) the determination of the mechanical properties of cuprous oxide formed by complete oxidation of copper, and (2) the determination of the mechanical properties of cuprous oxide in situ while still in contact with copper.

The results of study (1) are summarized in Appendix C. Many approaches to (2) are possible and after several approaches which were considered not sufficiently definitive, the method decided upon involves measurements of stress-strain of thin copper and oxidized copper films by following the deflection and bursting point under the application of a differential pressure. The method has been given the name the "bulge technique."

Because of the difficulty of adequately mounting and making grips on thin film samples, the bulge technique is advantageous for making measurements of mechanical properties. The sample to be tested is mounted over a hole and deformed by the application of a lateral pressure. While the applied pressure and the resultant deflection of the film are the experimentally measured quantities, it is necessary to relate the resulting stress-strain system in terms of the pressure and deflection in order to be able to determine mechanical properties from the experimental data. For this purpose the shape assumed by the deformed film is also necessary. A mathematical evaluation of the bulge technique is included in Appendix A in which the results and limitations of the theory are discussed. To supplement the theory an experimental evaluation

was made and is included in Appendix B. These evaluations are necessary in order to make a significant analysis of the experimental data.

In Appendix A it is shown that independent of the stress-strain mechanism, the pole stress in a bulged film is

$$T_o = p_o a^2/4tD \tag{1}$$

where p_o is the applied pressure, a the radius of the hole, t the film thickness, and D the central deflection of the bulged film. However, it is also shown that the relationship between pressure and strain and the central deflection is dependent upon the stress-strain mechanism, the boundary conditions of the problem, and the shape of the deformed film. In the experimental evaluation of Appendix B details are given to show that the shape of the film can be taken as a paraboloid. For this case and assuming a linear stress-strain relation (Hooke's Law), it is shown (Appendix A) that

$$p_o = x_2(Et/a^4)D^3 \tag{2}$$

$$\mathcal{E} = x_1(1-\nu)(D/a)^2 \tag{3}$$

where x_1 and x_2 are constants determined by boundary conditions, E is Young's Modulus, and ν is Poisson's ratio. For the most likely boundary conditions (see Appendix B) $x_1 = 3/4$ and $x_2 = 3$. It is to be emphasized that these relations should hold only for elastic behavior but would not hold if plastic behavior is included.

In eq. (1) the stress is computed from the experimentally observed pressure and deflection and is dependent upon the film thickness. The thickness can be eliminated by writing eq. (1)

$$T_o t = S = p_o a^2/4D \quad . \tag{4}$$

Eq. (3) shows that the strain is proportional to $(D/a)^2$ and this is true for elastic strain, plastic strain, or a combination of both. Thus, for analysis of the experimental data S can be plotted as a function of $(D/a)^2$. For the elastic region of the resulting curve, using eq. (2) and (3), S can be written

$$S = x_1 Et(D/a)^2 \tag{5}$$

with the slope being $(x_1 Et)$. A plot of this slope as a function of film thickness should indicate whether or not Young's modulus (or in general $x_1 E$) is a function of thickness. If the film is bulged to rupture, and the pressure and deflection at this point recorded, the breaking value of S and the breaking strength may be determined. A plot of this breaking strength as a function of thickness should indicate any thickness dependence in the strength of films.

EXPERIMENTAL

Sample Preparation

All copper films were deposited in a vacuum system at a pressure of approximately 10^{-5} mm Hg. The copper was evaporated from an electrically heated W basket or a W-wound BeO crucible. Depositions were made at room temperature onto glass slides coated with a thin layer formvar. The glass slides were masked to give a number of copper disc 1 cm in diameter. The evaporation time was varied in order to obtain a series of films of various thicknesses. Similarly the evaporation rate was held at approximately 500 A/min for one set of films and 4000-5000 A/min for another. Since depositions were made at room temperature all films were polycrystalline and of small grain size.

The purpose of the formvar coated slides is to allow removal of samples so that they can be mounted onto samples holders (Cu block containing holes approximately 0.75 mm radius) for the bulge apparatus. Initially samples were removed from the formvar-coated glass with ethylene dichloride, washed in alcohol, mounted on the sample holder, and stored in desiccators to dry. Better prepared samples were subsequently obtained by dissolving the formvar in chloroform (taking approximately three hours). The film, while still on the glass section, is lifted from the chloroform and transferred to the sample holder, which is barely immersed in ethyl alcohol, by a jet of alcohol from a hypodermic needle. The film is lined up over the test holes in the sample holder, carefully removed from the alcohol, and dried in a gentle stream of helium gas. The samples are then allowed to dry for twelve hours in covered containers so that no solvent remains between the film and the sample holder.

For investigation of oxidized copper films samples were prepared as described above and after mounting on the sample holder were introduced into an atmospheric oven at 150°C. The samples were allowed to oxidize for the desired time, 15 min to 72 hrs, removed from the oven, and allowed to cool before making bulge measurements. X-ray diffraction indicated that the films consisted of Cu and Cu_2O.

Thickness Measurements

Film thicknesses were measured with a polarization interference attachment to a Reichert Microscope. This is essentially a two beam instrument in which any phase difference introduced between the two beams causes a shift in the interference pattern formed on the test surface. Thus a step on

the surface, or edge of film, causes a shift in the pattern which is proportional to the step height (film thickness). The thickness is calculated from this fringe shift and the wavelength of light used (5830 A). However, in the case used here, the copper films are attached to formvar-coated glass so that reflection of one beam is from copper and the other from glass. A difference in phase upon reflection from these two surfaces will also produce a phase shift which is superimposed upon that due to the film thickness. This can be eliminated by coating the edge with some material; for example, silver. This overcoating can not be done on samples which are to be removed for bulge testing. Therefore a number of films of various thicknesses were measured on glass, overcoated with silver, and again measured. The results are shown in Table I. It

Table I. Film thicknesses of uncoated copper on glass and copper on glass overcoated with silver.

Uncoated thickness, A	Coated thickness, A	Difference, A
542 ± 50	920 ± 21	378 ± 54
610 ± 29	950 ± 54	340 ± 61
1140 ± 58	1570 ± 31	430 ± 66
1260 ± 32	1590 ± 53	330 ± 62
1370 ± 56	1630 ± 32	260 ± 65
2490 ± 77	2720 ± 48	230 ± 91
2490 ± 55	2820 ± 42	330 ± 88
	Average	328 ± 27

is seen that the coated thicknesses are greater than those uncoated. The deviations are those obtained from at least nine measurements. The average difference, 330 A, is then due to the difference in phase on reflection from glass and from copper. Since the phase shift for air-glass is π , the thickness difference leads to a phase shift of $.775\pi \pm .019\pi$ for air-copper.

This compares well with the phase shift, $.79\pi$, calculated from optical constants for evaporated copper films[1] at 6000A. Thus, the measured thickness of films to be used for bulge testing is increased by 330A to account for this. It was determined by measurements, also, that the formvar coating did not effect thickness measurements of uncoated samples.

Bulge Apparatus

The determination of shape and central deflection varies somewhat with the manner in which measurements are made. When depth measurements are made (either with a depth gauge or microscopically) measurements are made with respect to some initial point which may not be that corresponding to D = 0. For small deflections, this can cause considerable error. For this reason, measurements in this work are made, utilizing optical interference. A diagram of the experimental arrangement is shown in Fig. 1. Samples of films to be measured are mounted on a Cu block over holes which lead to a water aspirator for reducing the pressure on one side of the film. The difference in pressure between the two sides of the film is measured with a mercury manometer. The Cu block, with sample, is mounted onto a microscope stage and illuminated with Hg light (5461A) which replaces the regular light source. This light encounters a beam splitter which reflects the light to the sample through the objective of the microscope and allows the light reflected from the sample to pass to a micrometer eyepiece. The sample is partially covered with a thin glass cover slide so that interference occurs between light reflected from the film surface and the bottom side of the glass. Interference between these two

1. O. S. Heavens, Optical Properties of Thin Solid Films, (Butterworths Scientific Publications, London, 1955) p. 200.

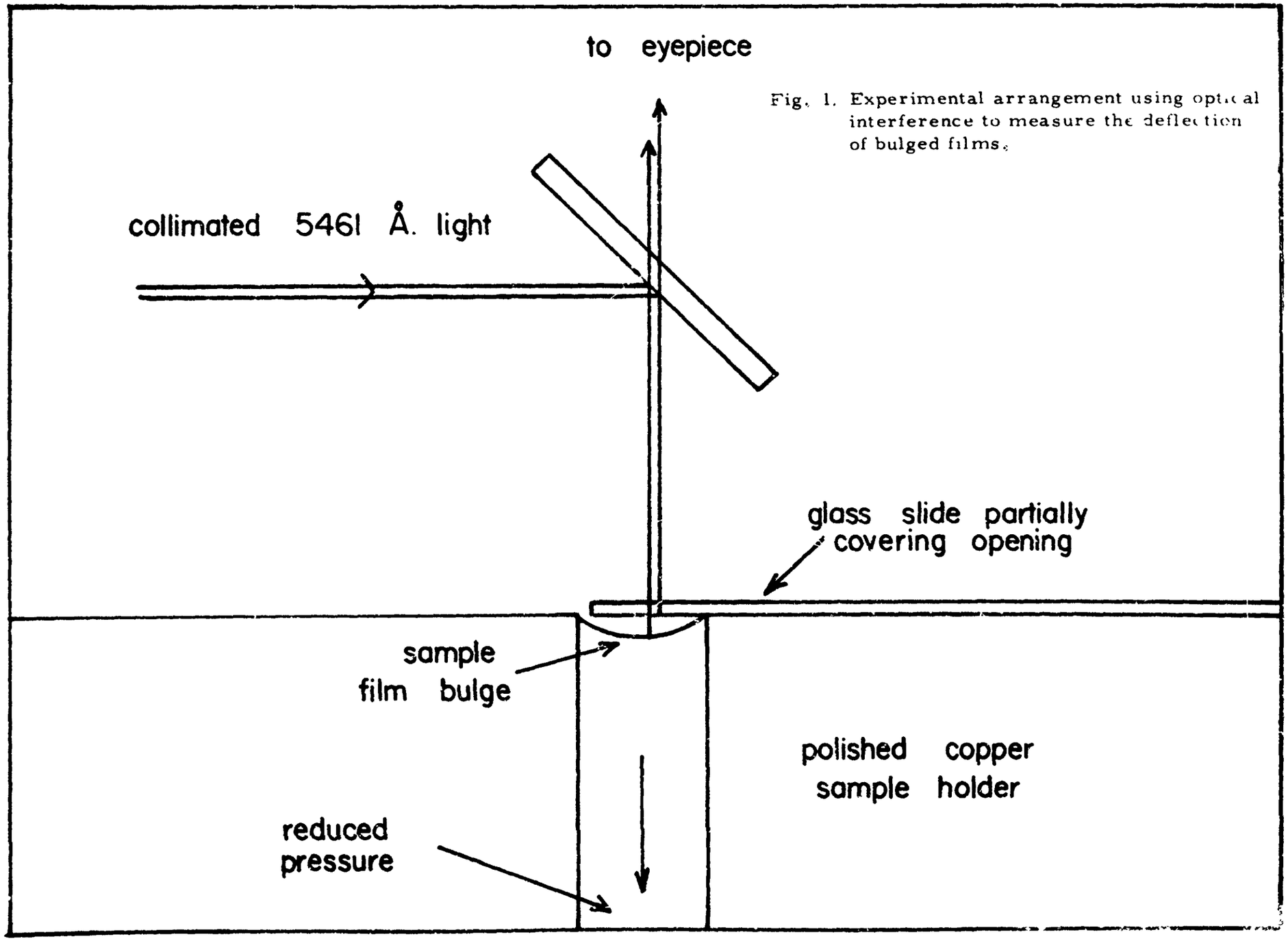

Fig. 1. Experimental arrangement using optical interference to measure the deflection of bulged films.

beams produces a set of interference fringes which represent paths of constant thickness between the sample surface and the bottom of the glass slide. For a symmetrically-bulged film, these fringes are circular and their spacing represents a distance change of $\lambda/2$; that is, a decreasing deflection of $\lambda/2$ for each fringe outward from the center. The radii of the fringes are measured with the micrometer eyepiece.

Results: Cu Films

Where possible the samples were mounted over several holes on the Cu block so that several runs were possible. In many cases the films were not initially flat but contained wrinkles around the edge of the hole or sagged into the hole. The films were deflected until the wrinkles were gone, if present, and circular fringes observed. The pressure was recorded and the diameter of the three central fringes measured in order to compute the central deflection as described in Appendix B for a parabolic shape. The pressure was then allowed to change slowly counting the number of fringes which appeared at the center. Since each fringe indicates an increased deflection of $\lambda/2$, the total central deflection corresponding to each pressure can be computed from the initial deflection. In many cases the diameters of the three center fringes were again measured and the central deflection computed and compared with that obtained from the previous deflection plus the change as determined by the number of fringes observed. In most cases the agreement was good, usually within several percent. After increasing the pressure until $(D/a)^2$ was a few tenths percent, it was reduced slowly and the number of fringes disappearing at the center were recorded for each pressure decrease. After several such

reductions the pressure was again increased in steps and the number of corresponding fringes recorded. This was continued up to the point where the films ruptured.

Films 700-5000 A thick were tested in the bulge apparatus in the manner described above. These included films deposited at low rates and high rates, approximately 500 A/min and 4000-5000 A/min, respectively. The values of S (proportional to the stress), computed from eq. (4), and the corresponding $(D/a)^2$ were obtained from the pressure and the deflection at each point. Typical curves of S as a function of $(D/a)^2$ for films of various thicknesses are shown in Fig. 2. The parameters S is used to eliminate thickness measurement errors and as a sort of normalization for comparison purposes. Since the strain is not all elastic and the exact expression for strain as a function of $(D/a)^2$ is not known (see discussion Appendix B), $(D/a)^2$ is plotted. It is observed that at the point where the pressure is released and then reapplied, that portion of the curve is linear, hence, involves only changes in elastic strain. The slope of this portion generally increases with increased film thickness. The last point on each curve represents the rupture point. For a given sample where more than one test could be made, or other samples deposited at the same time, the rupture point often varied. The variation was greater for thinner films and at times was as much as 20%. This is probably due to the fact that rupture did not occur at the center in all cases or defects in films caused weak spots and premature rupture. The values of S, as well as the rupture value, increase with decreasing thickness but not proportionally so that an increase in stress with decreasing thickness is indicated. It is also obvious from the curves of

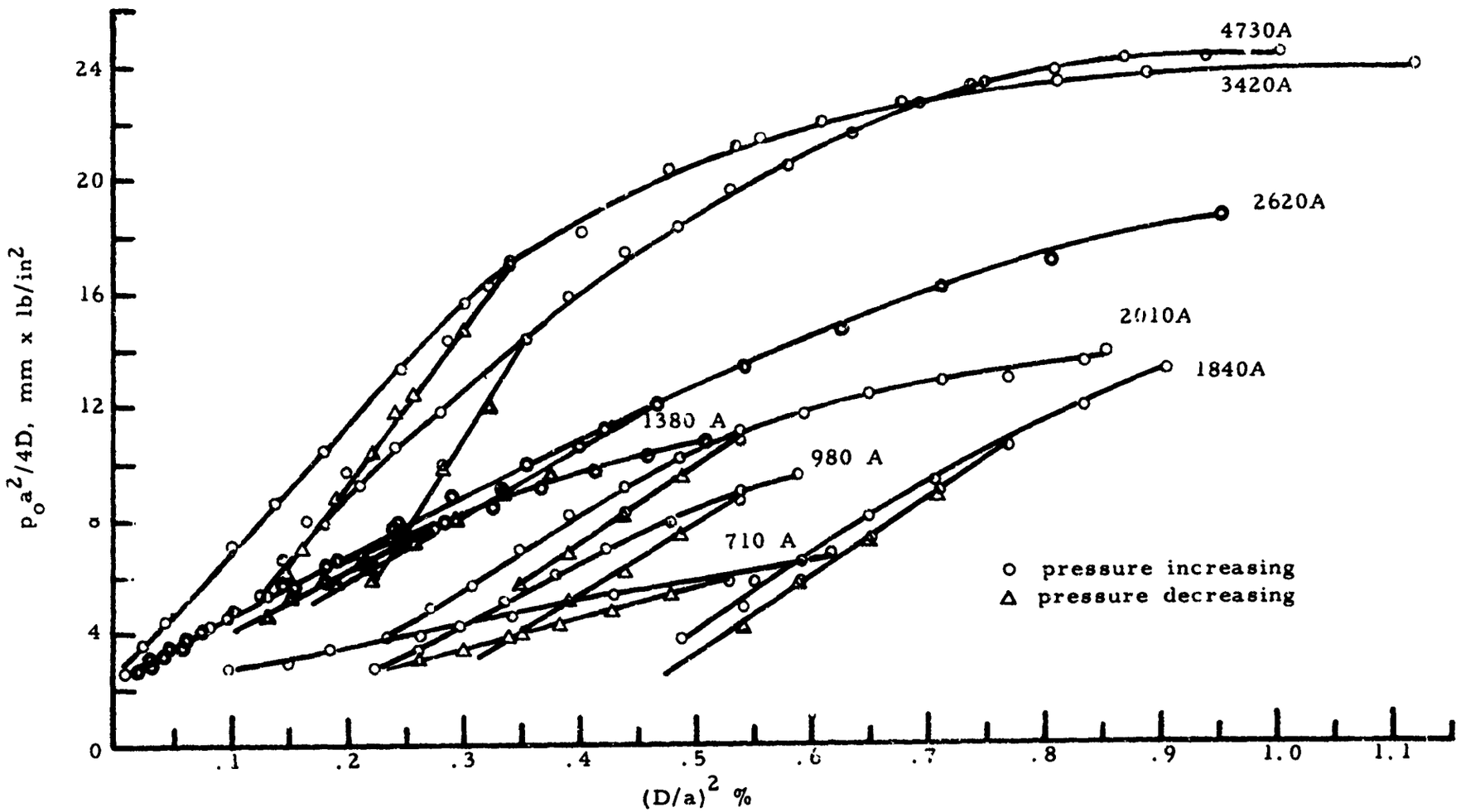

Fig. 2. Typical curves of $p_o a^2/4D$ as a function of $(D/a)^2$ for copper films of various thicknesses as measured by the bulge technique. Axis are proportional to stress and strain.

Fig. 2 that there is plastic behavior even at low stresses. At greater thicknesses the curves began to level off; that is, larger increases in strain occur for relatively small increases in stress.

Not all films tested were ruptured or the linear portion of the elastic behavior determined. However, of many samples tested, the average rupture value of S and the average slope of the elastic portion of the curves as in Fig. 2 are given in Table II for films of various thicknesses. The rupture (breaking) stress is also given as computed from S and the thickness. Separate films of

Table II. Thickness, average value of S, elastic slope, and rupture strength of copper films tested by the bulge method.

Thick. A	Rupture Value of S mm lb/in^2	Rupture Stress lb/in^2	elastic slope mm lb/in^2
710	6.1	86×10^6	1.08×10^3
900	8.42	86	2.36
1280	12.2	96	1.77
1375	10.3	75	2.20
1490	8.65	58	2.08
1550	10.7	69	2.29
1850	13.2	72	2.72
2010	14.6	73	2.80
2060	13.6	66	2.74
2130	15.4	72	3.50
2100	14.2	[illegible]	3.20
2370	16.0	68	3.16
2470	16.5	77	3.54
2530	17.3	68	
2580	17.3	67	3.[illegible]
2630	17.7	68	2.35
2660	18.6	70	
3080	21.0	68	4.75
3430	23.1	67	5.50
3980	24.0	60	5.60
4740	24.4	52	6.08
5070	28.8*	>58	6.40

* This film did not rupture at this maximum stress applied.

approximately the same thickness were not averaged. Thus, Table II gives some comparison of results on different evaporations and equal thicknesses. Such differences can be due in part to errors of thickness. The average values of S at rupture, S_r, from Table II are plotted as a function of the given thickness in Fig. 3. The point shown for the largest thickness indicated that the rupture point is above the plotted value since this film did not rupture at the maximum pressure which could be exerted. Although there are several points significantly off the curve (which can be caused by early rupture or thickness error), the curve appears linear. This curve has the form

$$S_r = A + Bt \qquad (6)$$

where B is the slope, equal to 61×10^3 lb/in^2, and A is the intercept, equal to 1.7 mm lb/in^2. Using eq. (4) the rupture stress can be written

$$T_r = B + A/t \qquad (7)$$

As the thickness becomes very large, T_r approaches B; hence, B represents the equivalent bulk breaking stress. This value of 61×10^3 lb/in^2 [illegible] be compared with a value of approximately 30×10^3 lb/in^2 for bulk copper. The average computed values of breaking stress from Table II are plotted in Fig. 4 in which the solid line is eq. (7) with the values of A and B given above. From this figure the breaking stress appears to increase significantly below approximately 1000 A. Above 1500 A the strength decreases only about 20%. The large deviations from this curve are similar to those in Fig. 3 and the majority appear to be due to premature rupture.

The average values of the elastic slopes, illustrated in Fig. 2 and given in Table II, are plotted as a function of thickness in Fig. 5. From eq. (5)

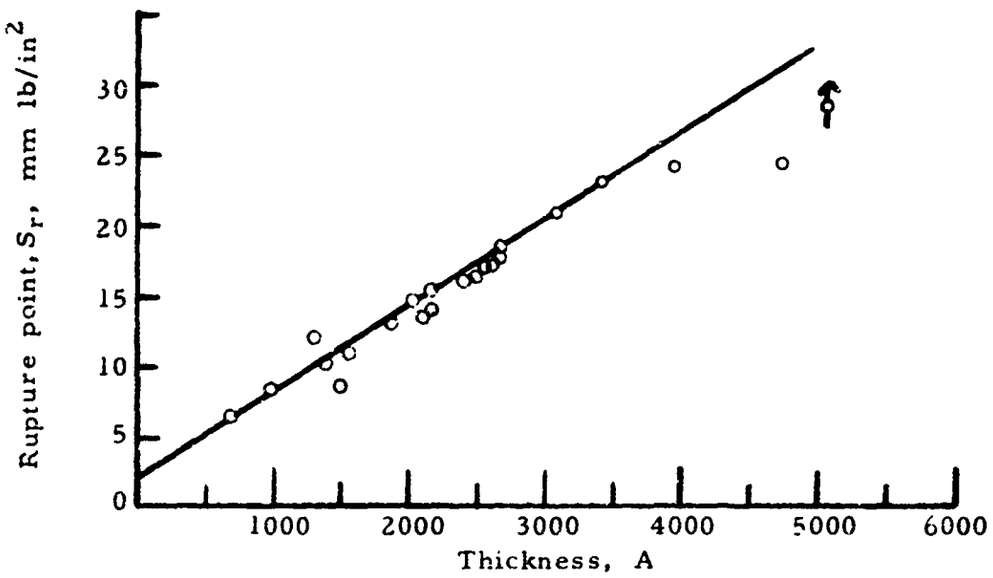

Fig. 3. Rupture point, S_r, of copper films as a function of film thickness.

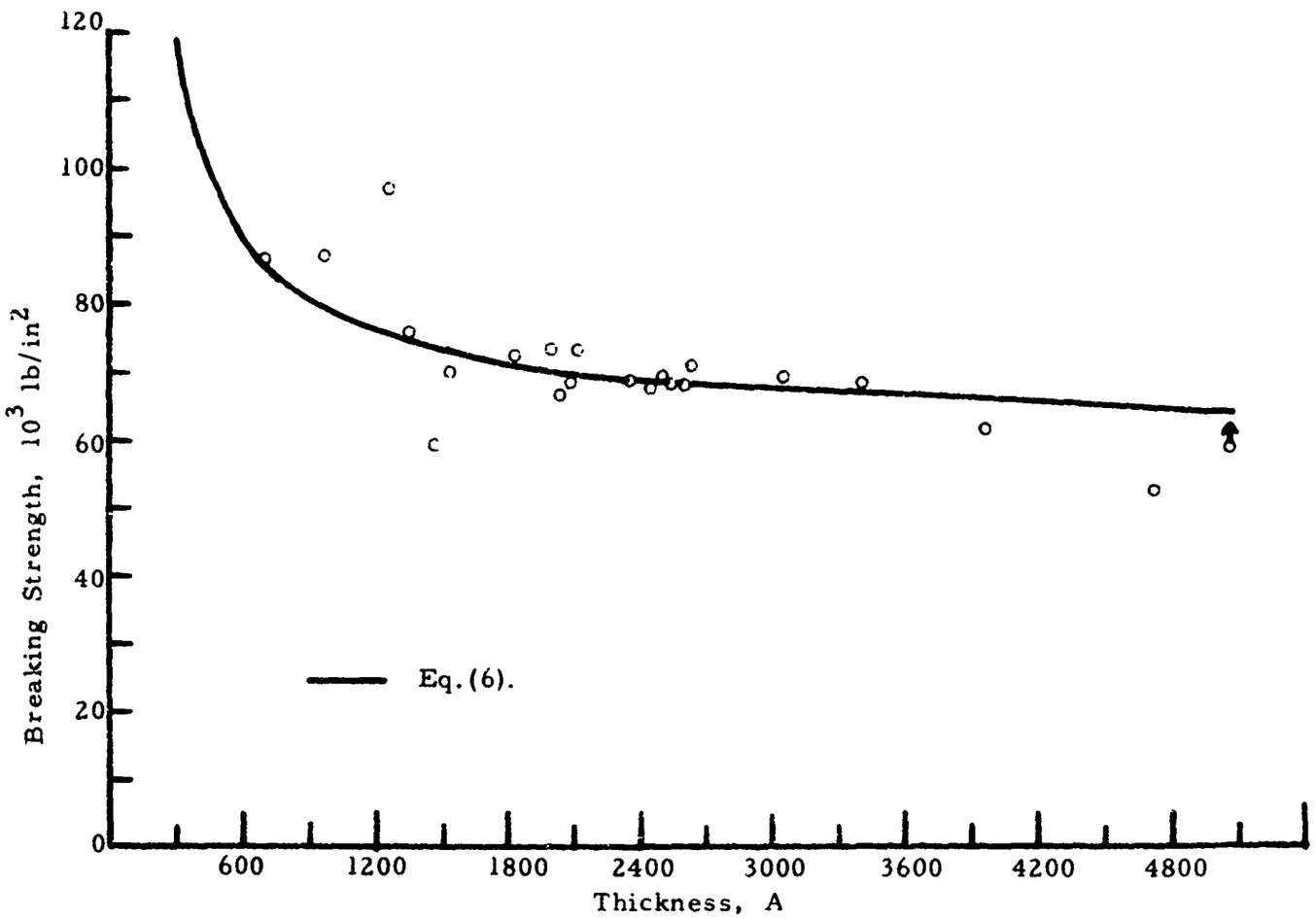

Fig. 4. Breaking strength of copper films as a function of film thickness.

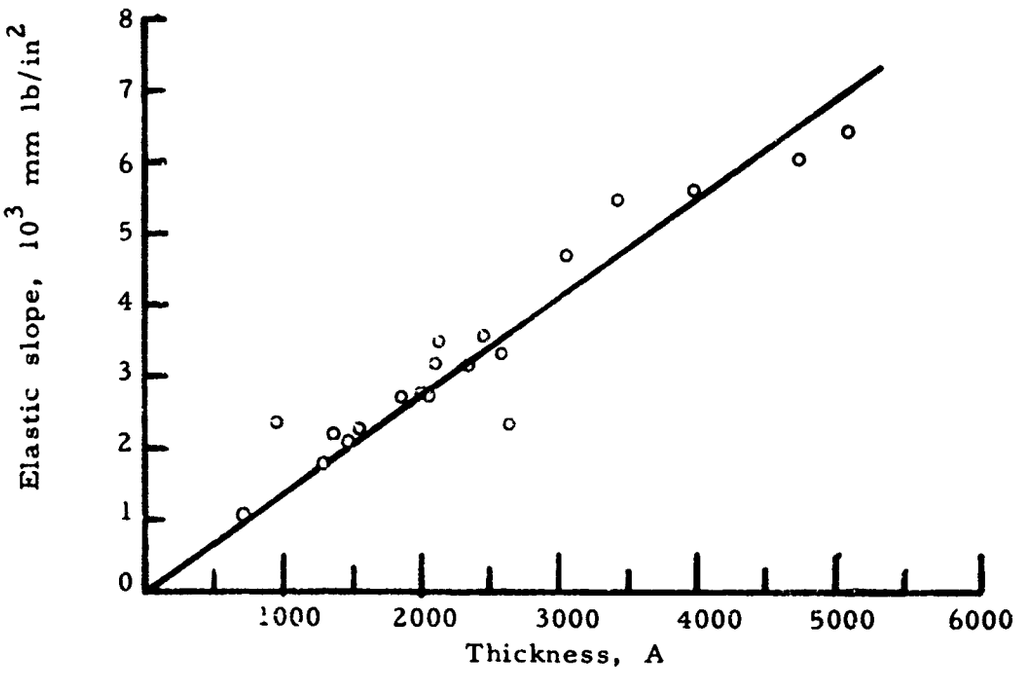

Fig. 5. Slope of the linear portion of curves such as in Fig. 2 as a function of film thickness.

this slope equals $x_1 Et$. These points are represented fairly well by a straight line through the origin. The slope of Fig. 5, then, is $x_1 E$ and is 13.8×10^6 lb/in^2. Using the value of x_1 most likely applicable as determined by experiment (see Appendix B), $x_1 = 3/4$, the value of Young's modulus is $E = 18.3 \times 10^6$ lb/in^2. This is to be compared to a value of 17.8×10^6 lb/in^2 for bulk polycrystalline copper. Fig. 5 indicates that Young's modulus is thickness independent. If E were thickness dependent the curve would not go through the origin nor be a straight line. This is contrasted to the increase in breaking strength with decreasing thickness.

Oxidized Cu Films

Many copper films were mounted onto the sample holder and oxidized as previously described. However, results of bulge testing were much more difficult to obtain. One reason for this was that upon oxidation many of the samples ripped or tore. Of those not torn, a large number were not oxidized uniformly as evidenced by differences in color across the film surface and the presence of "debri-like" spots, irregular in nature and number. The latter often appeared to occur at points where dust, residue, or "drying spots" were evident on the surfaces. There appeared more often for those films prepared by removal with ethylene dichloride. It was for this reason that other solvents were tried with chloroform giving the cleanest films. Even with the latter many were still torn upon oxidation and this or the nonuniformity of oxidation may be due to the known fact that oxidation may proceed from the surface inward at different rates and it was, in fact, observed on some films that at spots oxidation had taken place completely through the film. As a result of these

factors, it might be expected that rupture upon bulging would occur over a wide range of stresses. However, sufficient results have been obtained which allow comparisons to be made between unoxidized and oxidized films.

A number of films of essentially constant thickness, 1910 A, were oxidized for times up to 25 hours. Typical curves of S, computed from eq. (4), as a function of $(D/a)^2$ are shown in Fig. 6. The shapes of these curves are similar to those for the unoxidized films of Fig. 2. Thus plastic strain is present and a linear elastic region is obtained on reducing the pressure. The final point on each curve is the rupture point and the value of S_r is seen to decrease with increasing oxidation time. This is particularly obvious for the three curves which essentially overlap. The rupture point (S_r) for all films of this thickness are given in Table III. Although variations are observed the

Table III. Rupture point, S_r, and elastic slope of 1910 $\pm$ 70 A thick films for various oxidation times at 150°C.

oxidation time, min	Rupture point S_r, mmxlb/in^2	elastic slope 10^3mmxlb/in^2
5	13.2	2.72
15	11.8	2.00
	12.6	
60	11.2	2.14
	11.2	
120	11.1	1.58
240	8.6	2.00
960	10.7	4.36
	12.2	
	8.0	2.45
1500	4.8	

general trend is a decrease in rupture point. Since the thicknesses are constant, this means a decrease in rupture strength. From the observed

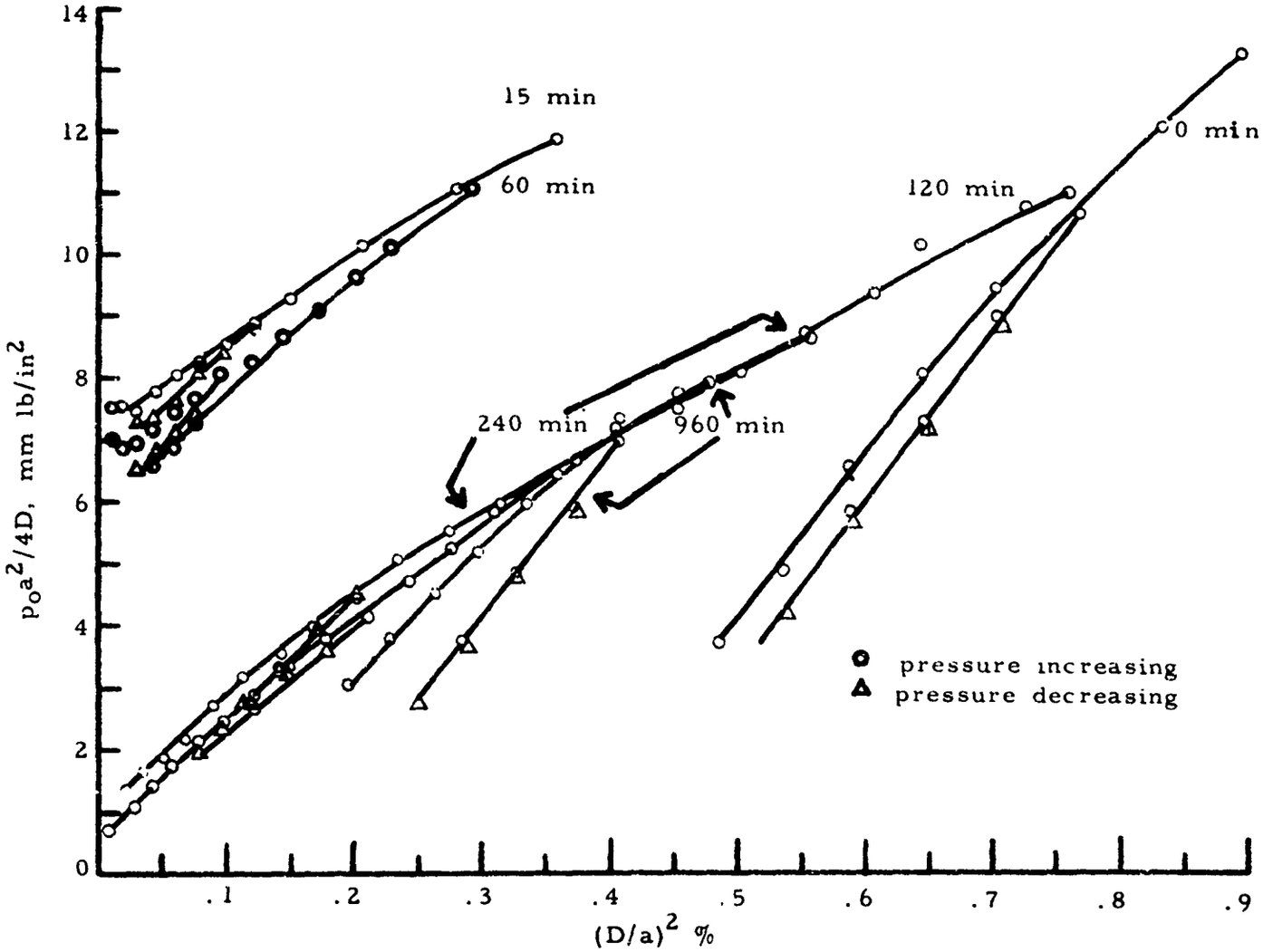

Fig. 6. Typical curves of $(p_o a^2/D)$ as a function of $(D/a)^2$ for 1910 A copper films oxidized at 150°C for various times.

values of the elastic slopes a defin. trend is not obvious.

Typical curves for a 15 min oxidation time at 150°C for several thicknesses are shown in Fig 7 The same general features are observed as in Figs. 2 and 6. The rupture point (not rupture strength, however) increases with thickness. Rupture values of S_r and the elastic slopes for all films oxidized 15 min are given in Table IV. Again the variations and agreements for various film samples are

Table IV. Rupture point, S_r, and elastic slopes of films of various thicknesses oxidized for 15 min at 150°C.

Thickness A	rupture point S_r, mmxlb/in^2	elastic slope 10^3 mmxlb/in^2
1130	4.5	1.25
	7.1	
1970	11.8	2.00
	12.6	
2205	12.2	1.33
	13.6	1.60
		2.00
2515	14.4	2.10
	13.6	2.00
2365	14.1	2.43
	15.7	2.32
	14.8	
2405	15.0	3.57
	16.9	3.40
2490	15.2	2.47
	15.8	2.53
4550	28.1	8.90
	27.8*	8.00
4760	24.4	4.00

* Maximum value, did not rupture.

seen with a general increase in the rupture value, S_r, with thickness. Likewise the elastic slopes increase with thickness although there are some large variations. In a similar manner typical curves of films oxidized for 4 hrs at 150°C and of

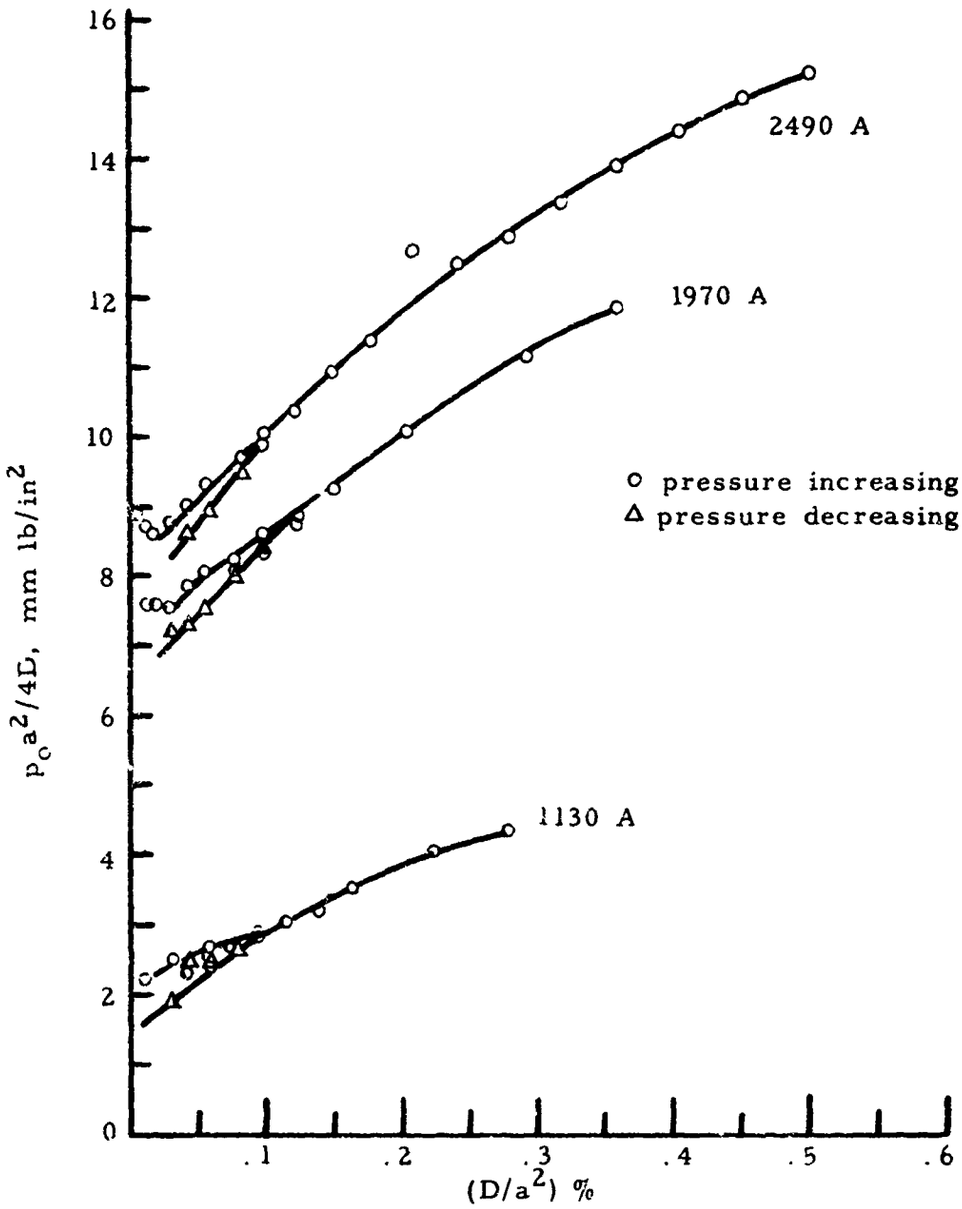

Fig. 7. Curves of $(p_o a^2/4D)$ as a function of $(D/a)^2$ for copper film of various thicknesses oxidized for 15 min at 150°C.

various thicknesses are shown in Fig. 8. The same general trends are again obvious. Table V gives the rupture point S_r and the elastic slope for all films of this series. The increase with thickness of the rupture point and a general increase in the elastic slope with thickness is again observed. The results

Table V. Rupture point, S_r, and elastic slopes of films of various thicknesses oxidized for 4 hr at 150°C.

Thickness A	Rupture point, S_r, mmxlb/in^2	elastic slope 10^3 mmxlb/in^2
1470	7.25	1.75
1870	8.65	2.00
2100	9.8	2.76
	9.3	2.06
	12.0	2.38
	11.3	2.59
2405	10.2	
	12.3	
2460	12.5	3.06
	16.9	2.45

for other oxidation times not included in Tables III, IV, or V are included in Table VI for comparison.

The rupture strength of the above oxidized films have not been given since the film thickness is necessary. The film thicknesses given are those of the unoxidized films. Since it was not possible to determine directly the amount of film oxidized (even assuming uniform oxidation), the films may consist of a copper layer and a copper oxide layer, or for sufficient times all oxide. Of course, for non-uniformly oxidized films the thickness of the two components cannot be separated. It is known that the thickness of an oxidized film increases. Thus, the thickness to be used in the computation of strength is in question. It was primarily for this reason that the quantity S of eq. (4) has been used since

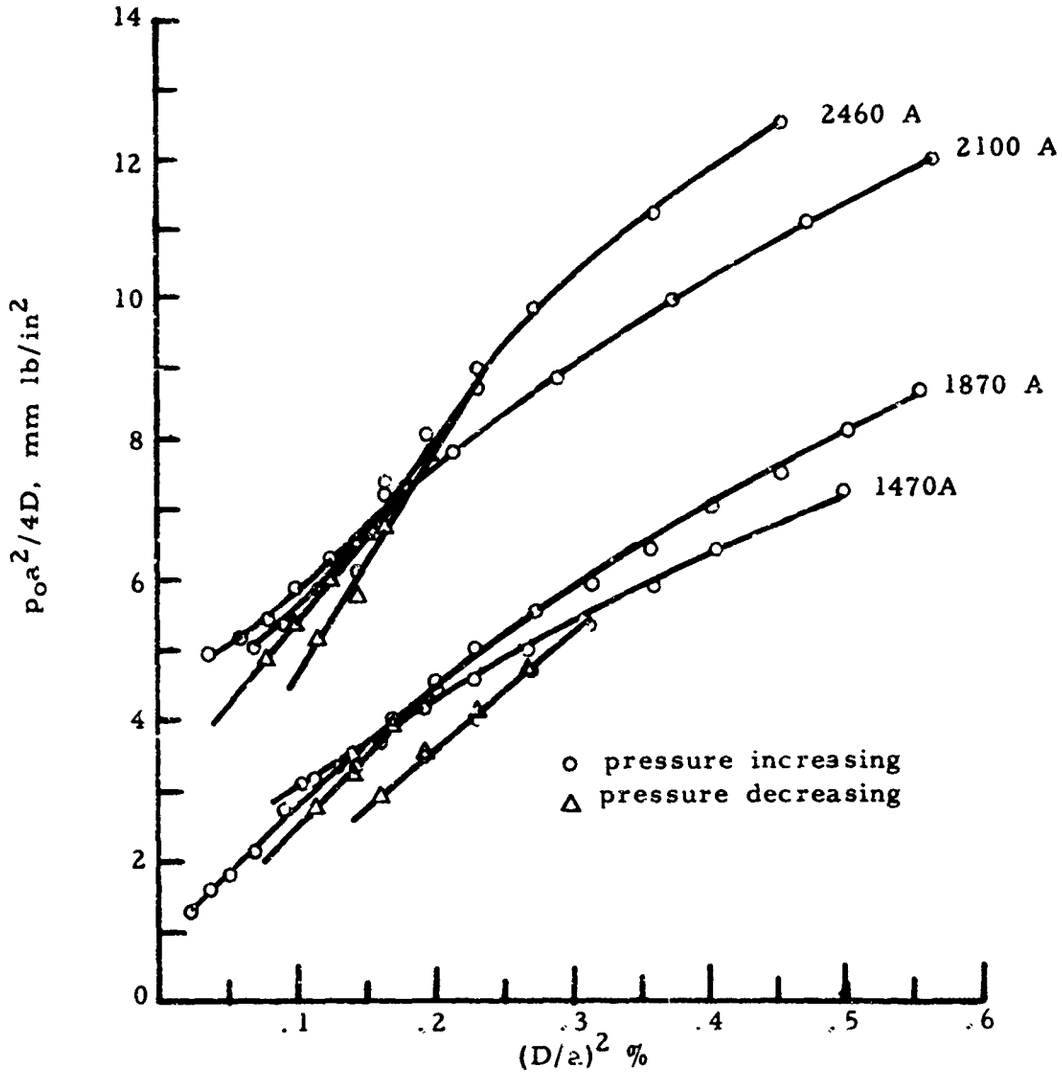

Fig. 8. Curves of $(p_o a^2/4D)$ as a function of $(D/a)^2$ for copper films of various thicknesses oxidized for 4 hrs at 150°C.

Table VI. Rupture point S_r and elastic slopes of films of various thicknesses and oxidized at various times at 150°C.

Oxidation time, min	thickness A	rupture point S_r, mmxlb/in^2	elastic slope 10^3 mmxlb/in^2
60	2010	8.6	1.85
	2090	10.6	
120	2060	12.0	
	2470	14.4	3.00
		14.3	2.25
165	980	5.3	
		7.1	
		6.4	
	2405	9.6	2.40
		10.6	
360	980	5.2	
	2500	14.6	
		11.7	
		13.7	
		10.4	
480	2030	14.4	2.94
1440	2390	10.0	
4320	3470	11.8	4.20
		10.9	4.50

the results can be compared directly from the data. For comparison, the rupture value, S_r, for the 15 and 4 hr oxidation times as a function of film thickness before oxidation are shown in Fig. 9. The line representing the unoxidized films is also shown. Although there is spread in the data it is seen that fairly good straight lines, parallel to that of the unoxidized films, can be drawn through the points. Thus, with the same slope the equivalent bulk strength is 61×10^3 lb/in^2 as for the unoxidized films. For increasing

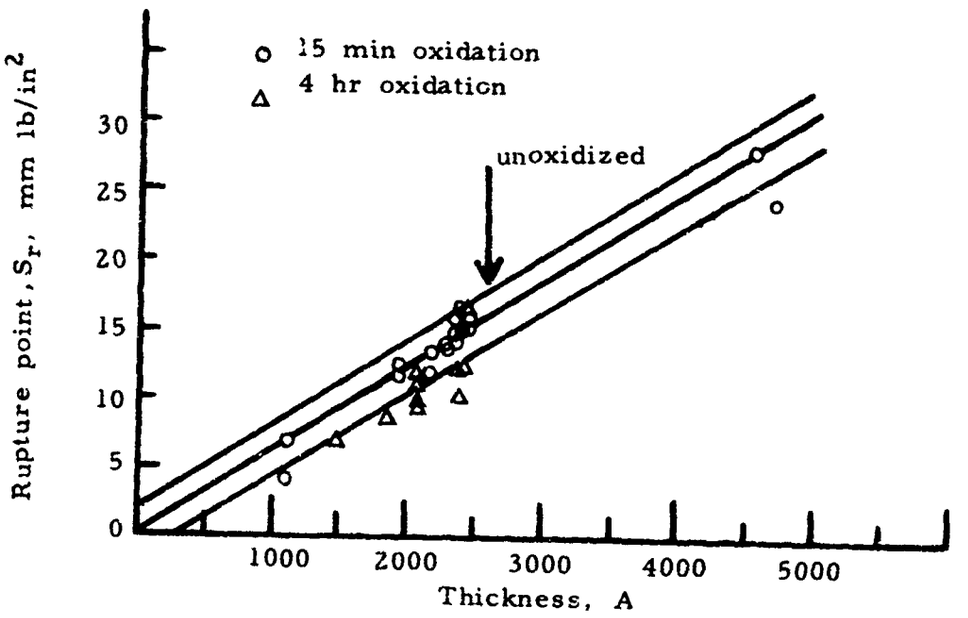

Fig. 9. Rupture point, S_r, of copper films oxidized for 15 min and 4 hr at 150°C as a function of film thickness.

oxidation time the values of S_r are shifted progressively lower. Each curve can be made to overlap the unoxidized curve by a shift to the right; that is, in the direction of decreasing thickness. For 15 min oxidation this shift is approximately 280 A and for 4 hr is approximately 580 A. The significance of this is that oxidation reduces the thickness of the remaining copper film and the properties measured are essentially those of the underlying copper. If this be the case, then for 15 min and 4 hr, respectively, the amount of copper oxidized is 280 and 580 A. Since the oxide lattice is approximately 18% larger than copper this would mean oxide films of 330 and 685, respectively. With oxidation on both sides of the film possible this indicates an oxide thickness of 165 and 342 A for 15 and 4 hr oxidation times, respectively. These values are to be compared to values of 175 and 340 A given by Young et al[2] for oxidation on (111) faces of copper at 159°C, but lower than for the (100) face. The spread in the data for the elastic slopes is too great for any comparison with that of the unoxidized films other than the values are lower indicating again a shift to thinner films, if the elastic modulus is essentially that of the unoxidized film.

CONCLUSIONS AND DISCUSSION

Measurement of the mechanical properties of copper films were performed primarily for comparison with results on oxidized films. The equivalent bulk strength of copper films was found to be 61×10^3 lb/in^2, approximately double that for bulk copper. The strength increases with decreasing thickness significantly only below 1000 A. In contrast to the

2. F. W. Young, J. V. Cathcart, and A. T. Gwathmey, Acta Met. 4, 145 (1956).

increasing strength, Young's Modulus appears to be reasonably independent of thickness. This fact is somewhat surprising in that generally it is expected that the breaking strength may be related to Young's Modulus. One conclusion from this may be that for sufficiently thin films the surface energy may increase with decreasing thickness, thereby requiring a larger force to separate two surfaces. These results also would be in agreement with those of Palatnik et al[3] which showed that for thicker films, 13-150 microns, the strength was independent of thickness.

It was mentioned in the experimental portion that films were deposited at two rates, one low and the other high. Sufficient films were not measured in order to state whether any rate effect was evident. This may be due to the fact that a rate dependence was only observed for low thicknesses[4].

It has been pointed out that difficulty was experienced in the testing of oxidized films. A large percentage were torn after oxidation. Also, the manner in which oxidation proceeds may introduce large scatter in the data and many films need be tested in order to establish completely significant relations. From the results obtained it appears reasonable that the mechanical properties of tested oxidized films are really those of the remaining unoxidized copper. If this be the case, such testing does not give information on the properties of the oxide itself except that its strength must be significantly less than that of copper. Of course, if oxidation is a patch-phenomena the above would be expected. The indications are that if uniform oxidation could be formed on surfaces the strength would not be impaired. Therefore, the

3. L. S. Palatnik and A. I. Il'enskii, Soviet Physics-Doklady 7, 832 (1963).
4. W. Kent Ford, Ph. D. Dissertation, University of Virginia. 1957.

effect which serves to impair surfaces is the action which causes oxidation to proceed non-uniformly with cracking resulting from localized stresses and hence renewed oxidation.

It is felt that bulge testing offers many advantages in obtaining mechanical properties of films in spite of some theoretical difficulties inherent in the problem. Also, better control of the oxidation process on the films could lead to more significant results. For example, effort to make and determine properties of completely oxidized films should be possible. Oxidation may be carried out under controlled action in a vacuum system where cleanliness of surfaces can be controlled.

ACKNOWLEDGMENT

Acknowledgment is made of the able technical assistance in preparing samples and making measurements by Mr. Harry Lanzillotti and Mr. Coleman Grandstaff. Acknowledgment is also made of the help of Mr. Calvin O. Tiller in preparing the early samples by vacuum evaporation and for many helpful discussions.

PUBLICATION AND TALKS RESULTING FROM RESEARCH.

A summary of the work was presented at the meeting of the Electrochemical Society in Chicago in October 1967 by Dr. H. Leidheiser. Dr. Billy W. Sloope will present a paper on the results at the Virginia Academy of Science meetings in Roanoke, Virginia, in May 1968. Preparation of the results for a publication is also in progress.

APPENDIX A

MATHEMATICAL EVALUATION OF THE BULGE TECHNIQUE

In order to determine stress and [illegible] in terms of the experimentally determined pressure and deflection for bulged film systems it is necessary to have theoretical relations between stress, pressure, and deflections. The shape of the deformed film is also of importance. Some of the theoretical results are presented and factors important for evaluation of the experimental results are discussed.

Relations between the stresses and the lateral pressure are obtained by considering the equations of equilibrium of the film. For a circular hole of radius a and the usual assumption that the deformation is symmetrical about the z-axis, a point on the film can be described by (r, θ), r being measured outward from the center of the hole and [illegible] (r) the vertical deflection. Letting T_1 and T_2 represent the mean values of the stress over the thickness for the r and θ-directions, respectively, the equation of equilibrium when no body forces act parallel to the middle surface of the film can be expressed as follows[1]:

$$\frac{d}{dr}\left(r T_1\right) = T_2 \quad , \quad T_1 + r\frac{dT_1}{dr} = T_2 \qquad . \qquad (1)$$

A stress function ϕ, satisfying eq. (1), is introduced such that

$$T_1 = \frac{E}{r}\frac{d\phi}{dr} \qquad T_2 = E\frac{d^2\phi}{dr^2} \qquad , \qquad (2)$$

1. J. Prescott, Phil. Mag. S 6 43, 97(1922).

where E is Young's modulus. For this case the stress in the z-direction is assumed negligible. When the deflections of the film are greater than the thickness t, the effect of T_1 and T_2 on equilibrium in z-direction must be considered. Prescott[1] showed that for this case, membrane theory, an additional equation of equilibrium becomes

$$\frac{1}{rT_1}\frac{d}{dr}\left(rT_1\frac{dw}{dr}\right) = \left(T_1\frac{d^2w}{dr^2} + \frac{1}{r}\frac{dw}{dr}\frac{d^2\phi}{dr^2}\right) = \frac{E}{r}\left(\frac{dw}{dr}\frac{d\phi}{dr} + \frac{dw}{dr}\frac{d^2\phi}{dr^2}\right) - p/t \quad . \tag{3}$$

Since the film surface is described by w(r), the principal radii are given by

$$-R_1 = \left(\frac{d^2w}{dr^2}\right)^{-1}, \quad -R_2 = \left(\frac{dw}{dr}\right)^{-1} \quad .$$

Thus equation (3) can be written

$$\frac{T_1}{R_1} + \frac{T_2}{R_2} = -p/t \quad . \tag{4}$$

If the shape of the deformed film is known so that the radii can be expressed from the geometry and p is assumed constant, eqs. (4) and (1) can be solved for T_1 and T_2 in terms of p. However, since eqs. (3) and (4) express equilibrium in the z-direction, p may be a function of r. In such cases, eq. (3) can be integrated to give

$$rT_1\frac{dw}{dr} = -r^2\frac{T_1}{R_2} = -\frac{1}{t}\int p\,r\,dr \quad . \tag{5}$$

Writing

$$T_1 = \cdot\left[1 + B_1(r) + B_2(r) + B_3(r) + \cdots\right] \quad , \tag{6}$$

performing the integration, and substituting into eqs. (5) and (1) one obtains

$$T_1 = \frac{p_0 R_2}{2t}\left[1 + \frac{2B_1}{3}\left(\frac{r}{a}\right) + \frac{B_2}{2}\left(\frac{r}{a}\right)^2 + \cdots\right] \quad (7)$$

$$T_2 = \frac{p_0 R_2}{2t}\left[\left(2 - \frac{R_2}{R_1}\right) + 2B_1\left(1 - \frac{R_2}{3R_1}\right)\left(\frac{r}{a}\right) + \cdots\right].$$

At r = 0,

$$T_{10} = T_{20} = T_0 \quad (8)$$

since $R_{10} = R_{20}$. There are several significant points concerning the relations between the stresses and the pressure. Eqs. (7) and (8) are independent of any particular stress-strain charac ristic, represent the total pole stress in the film, and can be determined from the applied pressure and pole radius.

As indicated above, the pole radius is needed to compute the stress. For this purpose the shape of the film is important. Generally, the shape of the film surface may be represented by

$$W(r) = D\left[1 - b_2\left(\frac{r}{a}\right)^2 + b_4\left(\frac{r}{a}\right)^4 + \cdots\right] \quad (9)$$

where D is the central, or maximum, deflection (r = 0). Differentiati eq. (9) with respect to r, the pole radius becomes R = $a^2/2Db_2$ and the pole stress P $a^2/4tDb_2$. It will be shown later (Appendix B) that the product Db_2 is essentially constant, equal to that for a spherical shaped surface. However, a further relationship is necessary in order to relate pressure and lection with the mechanical properties.

Since the pressure produces a deformation, the resulting strain needs to be described. In the coordinate system used, the two components of strain

may be written

$$\varepsilon_1 = \frac{du}{dr} + \frac{1}{2}\left(\frac{dw}{dr}\right)^2 \quad , \quad \varepsilon_2 = u/r \tag{10}$$

where u is the elongation in the r-direction. The term $\frac{1}{2}(dw/dr)^2$ must be retained since the deflections are assumed large compared to thickness while the second order change $(du/dr)^2$ can be neglected. It must be pointed out that these equations refer to an initial unstrained state whereas experimentally this may not be possible. Use of these forms requires knowledge of both u(r) and w(r) which are related to the shape of the deformed film.

In order to obtain information on the mechanical properties it is necessary to compare data to some stress-strain characteristics. For the case of elastic stress-strain Hooke's Law is assumed and the stress-strain relations may be written

$$\varepsilon_1 = \frac{1}{E}\left(T_1 - \nu T_2\right) \quad , \quad \varepsilon_2 = \frac{1}{E}\left(T_2 - \nu T_1\right) \tag{11}$$

where ν is the Poisson ratio. Substituting eqs. (2) into (11), differentiating, and combining with eqs. (10) in order to eliminate u and du/dr one obtains the relation

$$\nabla^4 \phi = -\frac{1}{r}\left(\frac{dw}{dr}\right)\left(\frac{d^2w}{dr^2}\right) = -\frac{1}{r}\left(\frac{d}{dr}\left[\frac{1}{2}\left(\frac{dw}{dr}\right)^2\right]\right) . \tag{12}$$

This equation and eq. (3), rewritten as

$$\frac{E}{r}\left[\frac{d}{dr}\left(\frac{dw}{dr}\frac{d\phi}{dr}\right)\right] = -\frac{p}{t} \quad , \tag{3}$$

contain three functions w(r), p(r), and ϕ(r) which can be found if one of them is known. Using w(r) given by eq. (9), eq. (3) can be solved by repeated

integration to obtain ϕ (r), and thus T_1 and T_2. Comparing these with eqs. (7) the constants B_i can be determined in terms of the b_i. However, such general solutions indicate little without knowledge of the constants and in addition the solutions involve arbitrary integration constants whose values are also necessary. These constants are determined by the boundary conditions of the particular problem. Herein lies the major problem in the interpretation of data on bulged films; that is, the conditions involved in the stress-strain experiment must be known in order to select proper relations for evaluation of experimental data. Therefore, the more general type of solutions will not be pursued. Instead the shape consistent with experimental data (Appendix B) will be assumed and solutions obtained which can then be further compared with experiment.

In Appendix B it is shown that the shape is closely that of a paraboloid (or an approximation of a sphere). The equation of the cross-section may be written $w = D[1-(r/a)^2]$, hence $R_r = a^2/2D$ and the pole stress of Eq. (8) becomes $T_o = P_o a^2/4tD$. Repeated integration of Eq. (12) gives for the stresses

$$T_1 = \frac{\psi_o E}{2} - \frac{ED^2}{4a^4} r^2$$
$$T_2 = \frac{\psi_o E}{2} - \frac{3ED^2}{4a^4} r^2 \tag{13}$$

where ψ_o is a constant of integration. At $r = 0$, $T_o = \psi_o E/2 = P_o a^2/4tD$. Hence,

$$T_1 = \frac{P_o a^2}{4tD} - \frac{ED^2}{4a^4} r^2$$
$$T_2 = \frac{P_o a^2}{4tD} - \frac{3ED^2}{4a^4} r^2 \tag{14}$$

We now require expressions for the strain and for w(p). This involves knowing the boundary conditions. Since the films are not clamped, and some evidence[2] indicates that even clamped films slip, the supported edge will be considered (for details see Appendix B). For the simply supported edge $T_1 = T_2 = 0$ at $r = a$. However, eqs. (14) indicate that both cannot be in this case. Thus it is assumed that the stress T_1 or T_2 is zero at $r = a$.

(1) Assume $T_1 = 0$, $r = a$. Then,

$$p = \left(E \, t/a^4 \right) D^3 \, . \tag{15}$$

This indicates that for the linear elastic case the deflection increases as the cube root of the applied pressure. This dependence is similar to that given in solutions by Timoshenko[3] and Tolkachnik[2]. By eq. (11) the pole strain is

$$\varepsilon_{r} = \varepsilon_{\theta} = \frac{1-\nu}{E} T_{r} = \frac{1-\nu}{E} \left(\frac{p a^2}{4 t D} \right) = \frac{1-\nu}{4} \left(D/a \right)^2 \, . \tag{16}$$

(2) Assume $T_2 = 0$ at $r = a$. Then,

$$p = \left(E \, t/a^4 \right) D^3 \tag{17}$$

which gives the same dependence between D and p as eq. (15). Finding the strain as in case (1),

$$\varepsilon_{r} = \varepsilon_{\theta} = \frac{2(1-\nu)}{9} \left(D/a \right)^2 \, . \tag{18}$$

---

2. S. V. Tolkachnik and V. U. Rostokinskii, Soviet Physics - Doklady 7, 246 (1962).
3. S. Timoshenko, Theory of Plates and Shells, (McGraw Hill Book Co., Inc., New York, 1940), p. 56.

Unfortunately, there is no information which will indicate which of these analyses are correct, if either. It does emphasize, however, the importance of knowing the boundary conditions in order to obtain proper relations for comparison with experimental data and to obtain mechanical properties. While the pole stress can be obtained, the strain is not uniquely determined. Nevertheless, these relations are useful for evaluation of experimental data.

APPENDIX B

EXPERIMENTAL EVALUATION OF BULGE TECHNIQUE

As indicated in the description of the experimental set-up, the applied pressure and the resultant deflection of the film are the experimentally measured quantities. Further, it was emphasized in Appendix A that the shape assumed by the film and the boundary conditions are also important in determining the stress and strain from the measured parameters.

Beams et al[1], Catlin et al[2], and Hill[3] assumed a spherical cap. Gerard and Papirno[4] measured the deflection at the pole and the quarter chord and using the general equation for a conic found the surface to be more nearly a paraboloid. Recently Halasz and Krause[5] investigated the shape of bulged thin aluminum foils using fairly large holes and found the shape changed with pressure. For $(D/a) > .1$ the shape was elliptic although the spherical and elliptic assumptions gave equally good approximations over the range of (D/a) and p used. In the interference technique used D, the central deflection, is not measured directly since the fringe spacing decreases with increasing radius and, toward the film edge becomes difficult to measure, or count accurately. Thus, D must be calculated from an assumed shape.

In order to determine the shape, the radii of fringes were measured from

---

1. J.W. Beams, Structure and Properties of Thin Films, John Wiley & Sons, Inc., New York, (1959) p. 183.
2. A. Catlin and W. P. Walker, J. Appl. Phys. 31, 2135 (1960).
3. R. Hill, Phil. Mag. 41, 1133 (1950).
4. G. Gerard and R. Papirno, Trans. Amer. Soc. Metals 49, 132 (1957).
5. S. T. Halasz and I. Krause, Mat. Sci. Engr. 2, 77 (1967).

the center outward to approximately (3a/). Hence, each point on the film was measured as distance above the center rather than below the edge; that is d = D-w. As an example of the analysis, one possibility considered was the parabola (the cross-section of the surface). The equation of the parabola is $w = D[1 - (r/a)^2]$ which can be written $d/D = (r/a)^2$, hence, $D = d\,(a/r)^2$. Since d_1, the distance above center for the first fringe, is not necessarily $\lambda/2$ due to the possible phase change on reflection at the film surface and the fact that adjustment cannot easily be made to make the center initially completely dark or a maximum of intensity, the radii of the first three rings were used to find an average d_1. From the above equation $d_{i+1}/d_1 = (r_{i+1}/r_i)^2$ and $d_i + 1 = d_i + \lambda/2$. The d_i for the first three rings were found by this method and an average taken to find D. Once D and d_1 were known, all other d's were obtained by adding $\lambda/2$ for each successive fringe and w = D-d plotted as a function of (r/a) as shown in Fig. 1. Using the calculated value of D, the parabolic shape is shown by the solid line of Fig. 1. Since the hole radius, a = .765 mm, $(D/a)^2 = .41 \times 10^{-3}$. It can be shown that for a spherical cap with the $(D/a)^2$ indicated, the difference between the spherical and parabolic arc is considerably less than experimental error. As a matter of fact the usual approximation for the sphere is just the equation of the paraboloid. The same is true if an elliptic section is assumed; however, this might not be the case for much larger deflections. Two other cases were assumed.

(1) The clamped edge, assuming that the solution for small deflection holds for large deflections (Timoshenko[6]), $w = D[1 - (r/a)^2]^2$. Applying the same

6. S. Timoshenko, Theory of Plates and Shells, (McGraw Hill Book Co., Inc., New York, 1940), p. 56.

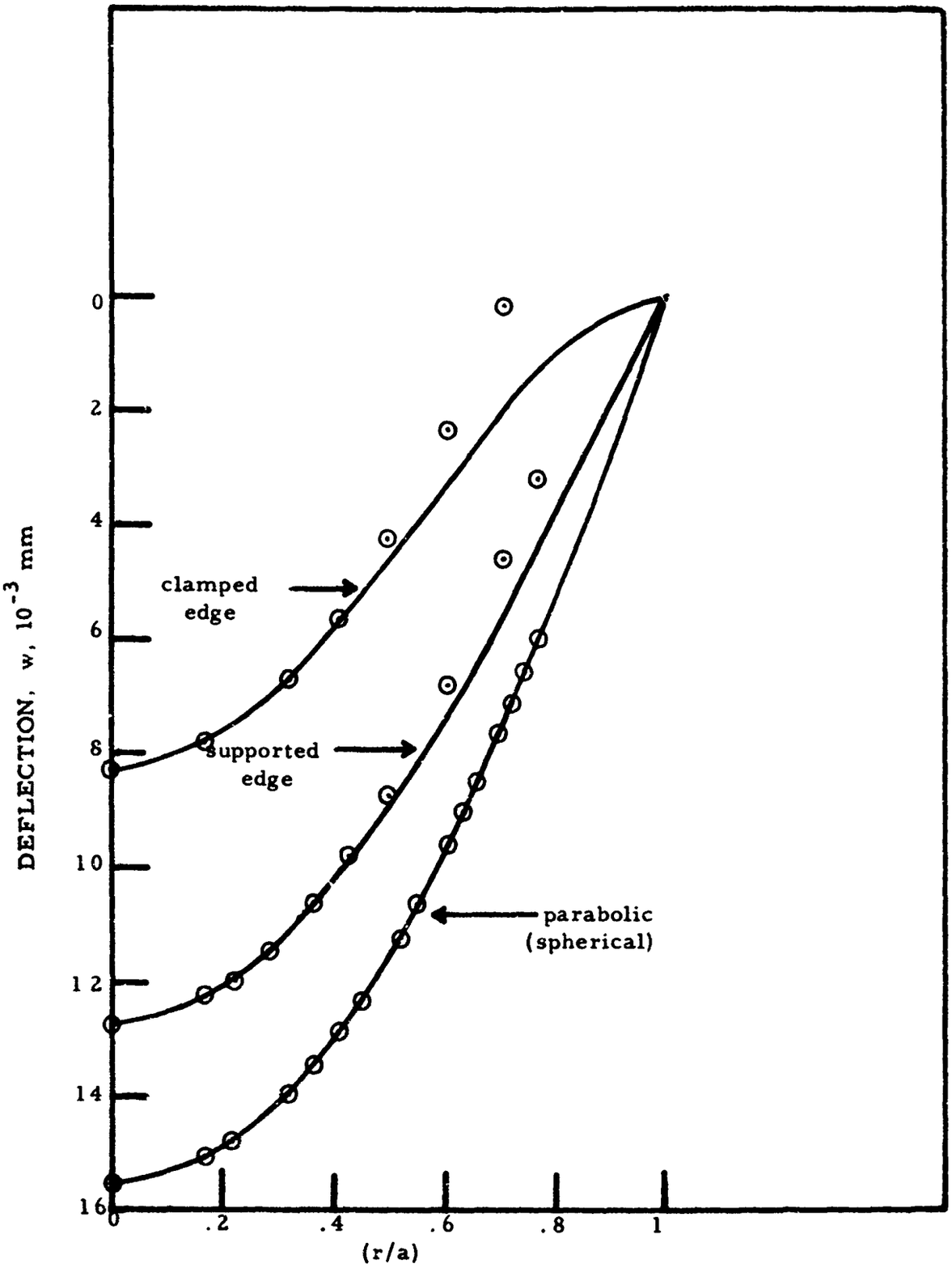

Fig. 1. Deflection of films as a function of distance from film center for several possible configurations.

analysis for the initial d_1 then $D = d_1/(r_1/a)^2[2-(r_1/a)^2]$. As for the parabolic case, D was computed and w plotted as a function of (r/a) from the above equation, again shown by the indicated solid line on Fig. 1. The values of w which would be indicated by the experimental data are also shown.

(2) The supported edge, under the same assumption as (1) was given a solution by Timoshenko[6] as

$$w = D\left[1 - \frac{2(3+\nu)}{(5+\nu)}\left(\frac{r}{a}\right)^2 + \frac{(1+\nu)}{(5+\nu)}\left(\frac{r}{a}\right)^2\right] .$$

Applying the same analysis, $D = d_1(a/r_1)^2/1.26[1-.206(r_1/a)^2]$, where ν has been set equal to 0.4 and makes little difference to the constants. The curve expected from the calculated D for this equation is plotted as the solid line on Fig. 1 and the deflections observed for given (r/a) also shown.

It is obvious that the experimental data follow the parabola (or sphere) more closely although near the center all three are closely matched. However, for the two solutions given by Timoshenko the maximum deflection D is too small for the number of fringes observed. In Appendix A it was indicated that the pole radius, $R_o = a^2/2Db_2$ was essentially a constant. The term Db_2 in the three cases above are 15.5, 16.5, and 16.0. Thus the pole radius can be approximately $R_o = a^2/2D$, where D is that for the parabolic case. As the pressure is changed, D changes, but all conics are essentially indistinguishable as long as (D/a) remains small. For the films measured (D/a) $\lesssim$ 0.1, hence the parabolic form appears to be useful.

In the case of Beams et al[1] and Catlin et al[2] the strain was taken as $2/3(D/a)^2$ which assumed an initially flat surface and a constant strain over the

surface. However, it can be easily shown that this is the average strain over the surface. According to Hill[3] the pole strain is $(D/a)^2$. If an initial deflection D_i (whether it be strain or not) is present, Catlin et al[2] consider the added strain as $2/3[(D/a)^2 - (D_i/a)^2]$. These, however, assume that the edges of the films are fixed; that is, clamped. Papirno[7] measured the pole deflection and the pole strain (with an attached strain gage) and found the strain was approximately $0.3(D/a)^{1.9}$ although a power of two is not inconsistent with the spread in their data. Appendix A emphasized that a factor to be considered in attempting to determine strain from the shape is the boundary condition; that is, the nature of the edges of the film (at $r = a$). There are two possibilities of interest, the clamped and the simply supported cases. For the clamped case the edges are fixed, which requires $u = 0$ at $r = a$. This is not the case for the supported edge, hence a sort of slipping or sliding takes place and the boundary condition needs to be otherwise described. Tolkachnik et al[8], investigating clamped glass films, found that the data indicated a sliding type edge. The significance of this is that for equal pressures a larger deflection will occur with supported edges than with clamped edges. This is seen to be the case in Fig. 1. Thus it is to be expected that the strain is a smaller fraction of $(D/a)^2$. This could explain the lower values of strain found by Papirno[7] than predicted by the usual formula.

As in the case of film shape, comparison with experimental data is useful in determining which boundary case is most likely. To do this eqs. (15, (16), (1[illegible]), and (13) of Appendix A can be generalized as

7. R. Papirno, J. Appl. Phys. 32, 1175 (1961).
8. S. V. Tolkachnik and V. U. Rostokinskii, Soviet Physics - Doklady 7, 246 (1962).

$$p_o = x_2(Et/a^4)D^3$$
$$\mathcal{E}_o = x_1(1- \quad)(D/a)^2 \qquad (1)$$

where x_1 and x_2 are constants dependent upon the choice of boundary conditions. Their values are given in Table I for a parabolic shape and for the clamped edge

Table I. Boundary condition constants and corresponding values of Young's Modulus from experimental data. Parabolic shape cross-section of deformed film assumed.

slope, Fig. 2 $lb/in^2/mm^3$		clamped edge	supported edge Case I	Case II
	x_1	$(1-\nu)^{-1}$	1/4	3/4
	x_2	$4/(1-\nu)$	1	3
1.26×10^4	E_1 (lb/in^2)	9.9×10^6	61.1×10^6	20.4×10^6
1.98×10^4	E_2 "	8.6 "	53	17.7
3.02×10^4	E_3 "	8.2 "	50.5	16.8
5.80×10^4	E_4 "	10.4 "	64.1	21.3
	$\mathcal{E}_o$	$(D/a)^2$	$.162(D/a)^2$	$.488(D/a)^2$

and the supported edge with the two cases given in Appendix A. Although the films are not clamped in the experimental test, this case is included for comparison. Since these equations were derived assuming elastic behavior, for comparison with experimental data p and D must be taken in a linear stress-strain region. This is accomplished by increasing p and D so that the films are under stress and strain. The pressure is then reduced in successive steps and the corresponding deflection determined as previously described. In this manner only the elastic strain is relieved. The pressure as a function of D^3 in this region is plotted in Fig. 2.for several films with thicknesses between 700 and 3000 A. These curves are seen to be linear in accordance with eq. (1) and the slopes, $x_2(Et/a^4)$, are given in Table I. From these slopes the corresponding

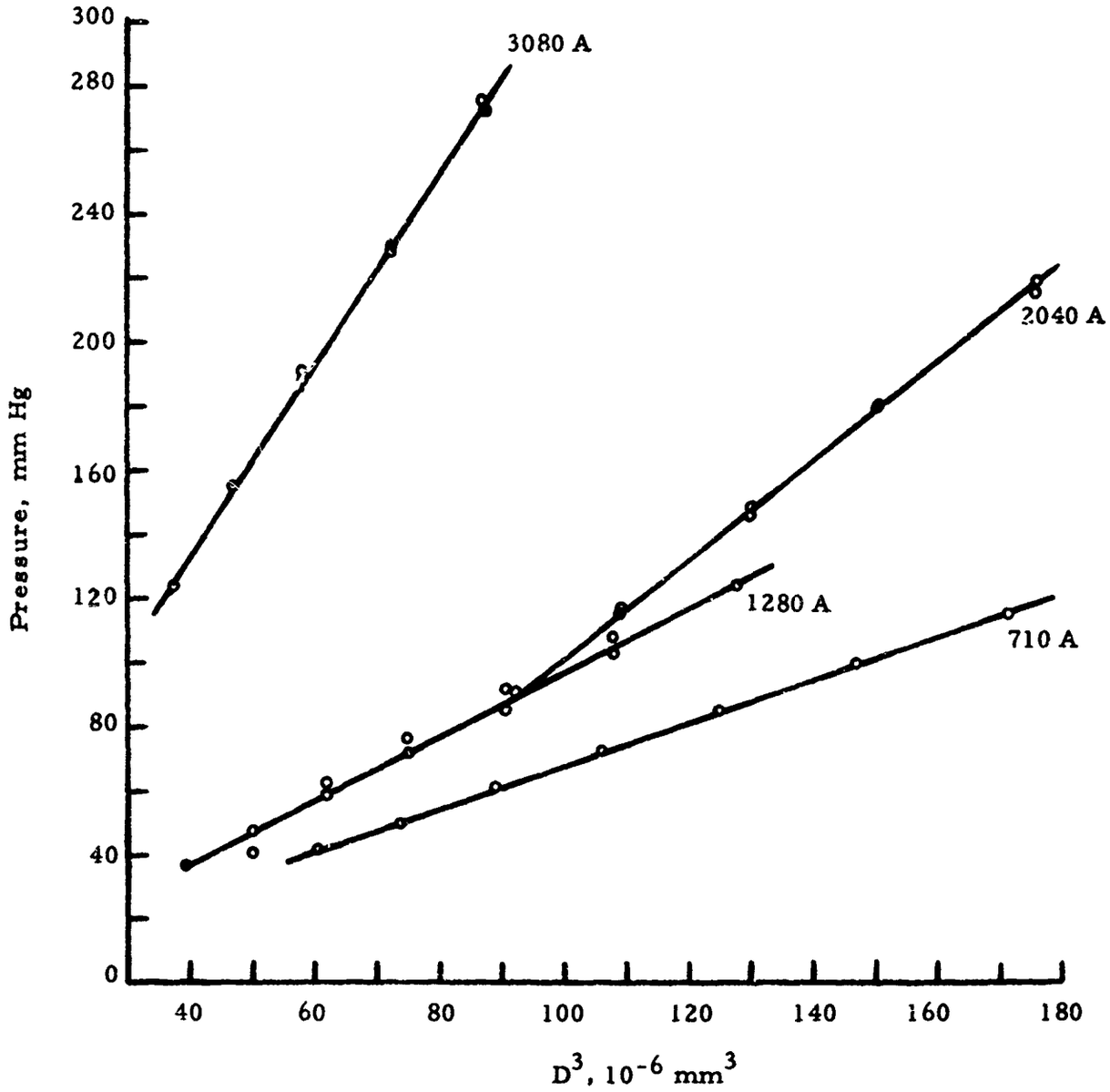

Fig. 2. Pressure as a function of the cube of the deflection in the elastic region for bulged copper films of various thicknesses.

values of Young's Modulus, E, are computed for the boundary values of x_2 indicated. It is seen that case II of the supported edge leads to values in better agreement with bulk copper, 17.8×10^6 lb/in^2, while the other cases are greatly different. Where necessary for computations ν has been taken as 0.35.

The corresponding expressions for strain in terms of $(D/a)^2$ are also given in Table I for the different boundary conditions. However, these expressions could be expected to be valid only during elastic stress-strain behavior. Thus, when plastic behavior is also present the total strain is increased and the corresponding deflection increased. In such a case, the constant x_1 should be smaller.

APPENDIX C

Mechanical Properties of Oxidized Single Crystal Copper

Massive single crystals of Cu_2O were prepared by the controlled oxidation of Cu single crystals. Large single crystals of copper, 2 to 3 mm thick and up to several square centimeters in area, were polished, cleaned, and placed in a Burrell Furnace for oxidation. Oxidation was carried out at 1000°C for periods of 42 to 48 hrs and the temperature was then increased to 1100°C and held for 48-64 hrs. Single crystal test specimens of Cu_2O were cut from these samples.

Mechanical properties of the Cu_2O single crystals were determined on an Instron testing machine. The modulus of elasticity under compressive conditions ranged from 189,000 to 232,000 lb/in^2 and the tensile strength under compressive conditions ranged from 18,500 to 89,000 lb/in^2 with an average value of 47,600 lb/in^2. Under transverse testing conditions, the modulus of elasticity ranges from 23,800 to 68,300 lb/in^2 with an average of 48,900 lb/in^2. The tensile strength under transverse testing ranged from 6840 to 8900 lb/in^2 with an average of 8030 lb/in^2. These results confirm the general observations made with brittle materials in that a wide range of values are obtained dependent upon the method of testing and the surface conditions of the samples.

Microhardness measurements were made on a large number of samples. Measurements were made in air, water, and in mineral oil. The hardness values ranged from 203 to 219 on the Vickers scale. No significant difference was noted between samples or between different crystals in the same sample. A similar range of values was obtained in the three environments used.

Unclassified

Security Classification

DOCUMENT CONTROL DATA - R & D

(Security classification of title, body of abstract and indexing annotation must be entered when the overall report is classified)

1 ORIGINATING ACTIVITY *(Corporate author)* Virginia Institute for Scientific Research, P. O. Box 8315 Richmond, Virginia 23226	2a. REPORT SECURITY CLASSIFICATION Unclassified 2b. GROUP

3 REPORT TITLE

MECHANICAL PROPERTIES OF THE CORROSION PRODUCT FORMED DURING OXIDATION OF COPPER.

4 DESCRIPTIVE NOTES *(Type of report and inclusive dates)*

FINAL REPORT

5 AUTHOR(S) *(First name, middle initial, last name)*

Billy W. Sloope

6 REPORT DATE 2 April 1968	7a. TOTAL NO OF PAGES 43	7b. NO OF REFS 15
8a CONTRACT OR GRANT NO ONR Contract No. N00014-66-C0182 b. PROJECT NO NR 036-066 c d	9a. ORIGINATOR'S REPORT NUMBER(S) Project #94 - Final Report 9b. OTHER REPORT NO(S) *(Any other numbers that may be assigned this report)*	

10 DISTRIBUTION STATEMENT

Distribution of this document is unlimited.

11 SUPPLEMENTARY NOTES	12 SPONSORING MILITARY ACTIVITY Office of Naval Research

13 ABSTRACT

The mechanical properties of copper and oxidized copper films have been measured using the bulge technique. The mechanical strength (rupture) was found to increase with decreasing thickness with a significant increase occurring below 1000 A. Young's Modulus is independent of thickness over the 700-4500 A thickness range. Copper films were oxidized in air at 150°C for times from 15 min to 72 hrs. Comparison of these results indicate that the mechanical properties observed are due to the remaining underlying copper film.

DD FORM 1 NOV 65 1473

Unclassified

Security Classification

Unclassified
Security Classification

14 KEY WORDS	LINK A ROLE	LINK A WT	LINK B ROLE	LINK B WT	LINK C ROLE	LINK C WT
Mechanical Properties						
Thin Films						
Copper						
Oxidized Copper						

Unclassified
Security Classification